

## Noise, Coherent Fluctuations, and the Onset of Order in an Oscillated Granular Fluid

Daniel I. Goldman,\* J. B. Swift, and Harry L. Swinney†

Center for Nonlinear Dynamics, The University of Texas at Austin, Austin, Texas 78712, USA

(Received 31 July 2003; published 29 April 2004)

We study fluctuations in a vertically oscillated layer of grains below the critical acceleration for the onset of ordered standing waves. As onset is approached, transient disordered waves with a characteristic length scale emerge and increase in power and coherence. The scaling behavior and the shift in the onset of order agrees with the Swift-Hohenberg theory for convection in fluids. However, the noise in the granular system is an order of magnitude larger than the thermal noise in the most sensitive convecting fluid experiments to date; the effect of the granular noise is observable 20% below the onset of order.

DOI: 10.1103/PhysRevLett.92.174302

PACS numbers: 45.70.Qj, 05.40.Ca, 45.70.Mg, 47.54.+r

Recent experiments [1] and simulations [2] on flows of dissipative granular particles have been found to be described by hydrodynamic theory, although the granular systems exhibit much larger fluctuations than fluids—a single wavelength in a pattern in a vibrated granular layer might contain only  $10^2$  particles instead of the  $10^{22}$  particles in one wavelength of a pattern in a vibrated liquid layer. Thus fluctuations play a more significant role in granular systems than in fluid flows. In fluids the fluctuations are driven by thermal noise and are described by the addition of terms to the Navier-Stokes equations [3,4]. This fluctuating hydrodynamic theory has been found to describe accurately the dynamics near the onset of a convection pattern in a fluid [5–8]. Here we describe an experimental study of fluctuations near the onset of square wave patterns in an oscillated granular layer, and we demonstrate the applicability of fluctuating hydrodynamics to this inherently noisy system.

**Experiment.**—We study a vertically oscillating layer of  $170\ \mu\text{m}$  stainless steel particles as a function of  $\Gamma$ , the peak plate acceleration relative to gravity; the container oscillation frequency  $f_d$  is fixed at 30 Hz [9]. The layer (depth five particle diameters) fluidizes at  $\Gamma \approx 2$  [10], and a square wave pattern with long-range order oscillating at  $f_d/2$  emerges at  $\Gamma \approx 2.77$ . The layer is illuminated at a low angle, and images are recorded on a  $256 \times 256$  pixel charge-coupled device (CCD) camera. We assume following [10] that for small amplitude disturbances the fluctuations in light intensity in the images are proportional to fluctuations in the layer density [11].

**Coherent fluctuations.**—Fluctuations are evident in the snapshot of the layer shown in Fig. 1(a). Spatial coherence with no orientational order is revealed by the ring in the spatial power spectrum  $S(k_x, k_y)$  shown in Fig. 1(b). The increase in the spatial and temporal coherence and the power of the fluctuations with increasing  $\Gamma$  is illustrated in Fig. 2, where insets with each spectrum  $S(k_x, k_y)$  show the corresponding azimuthally averaged structure factor,  $S(k) = \langle S(k_x, k_y) \rangle_\theta$  with  $k = \sqrt{k_x^2 + k_y^2}$ . [There is slight ( $< 1\%$ ) hysteresis in all measured quantities between

increasing and decreasing  $\Gamma$ , but we discuss only increasing  $\Gamma$ .] The power of the dominant mode increases while the width of the mode decreases with increasing  $\Gamma$  [12]. The fluctuations are readily visible at  $\Gamma = 2.2$ , which is 20% below the onset of long-range order. In high sensitivity measurements on Rayleigh-Bénard convection in  $\text{CO}_2$ , fluctuations became measurable only at 1% below the onset of convection [6], but a recent *tour de force* experiment on convection in  $\text{SF}_6$  near the critical point

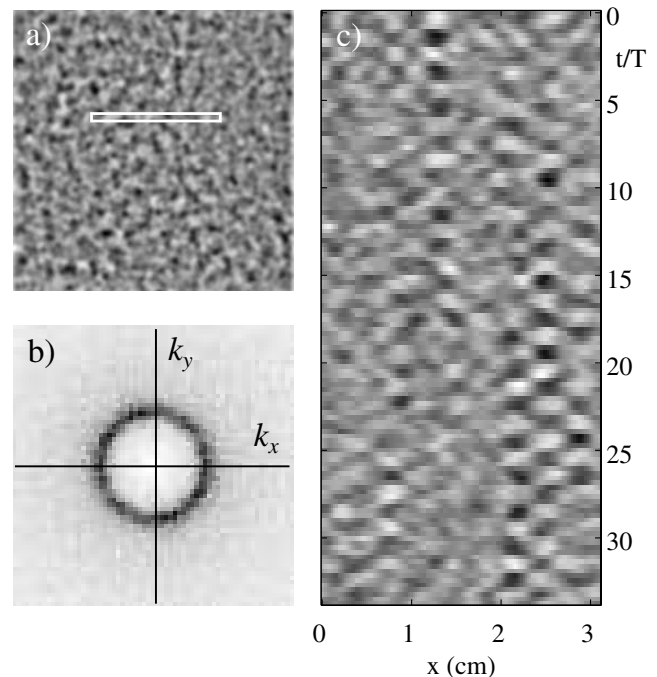


FIG. 1. (a) Snapshot of an area  $6.25 \times 6.25\ \text{cm}^2$  in a container oscillating with  $\Gamma = 2.6$ . (b) The spatial power spectrum of (a) has an intense ring corresponding to randomly oriented spatial structures with a length scale of  $0.52\ \text{cm}$  (100 spectra were averaged to obtain the spectrum shown). (c) Space-time diagram for the row of pixels in the box in (a); the period of the localized transient oscillations is  $2T \equiv 2/f_d$ .

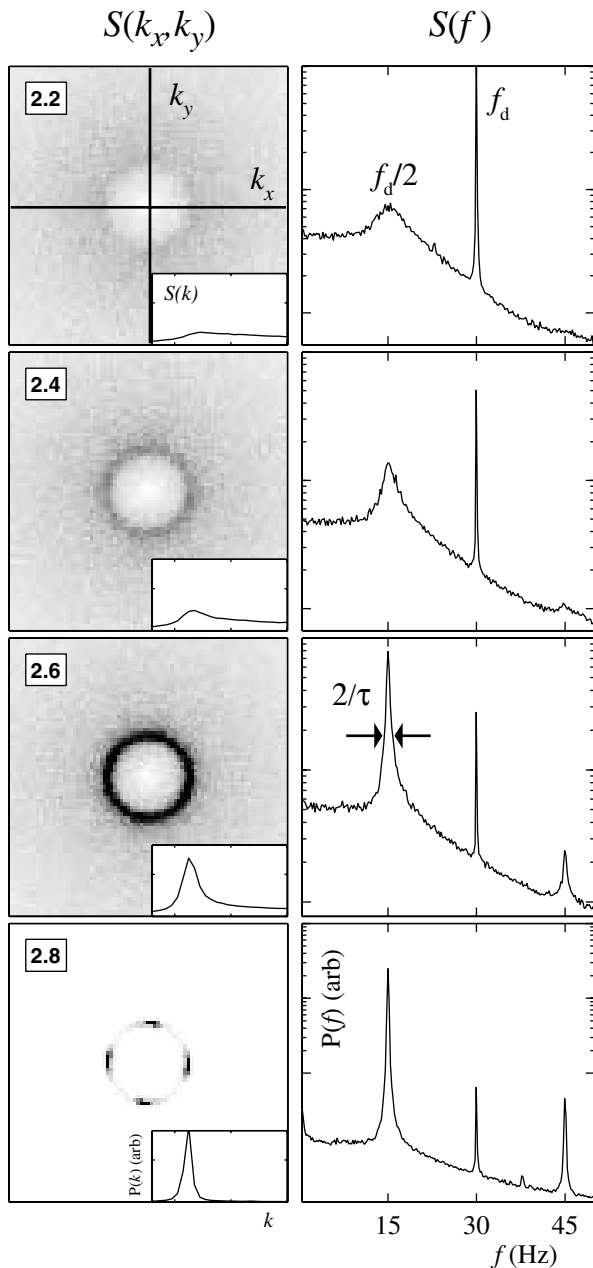


FIG. 2. Spatial power spectra  $S(k_x, k_y)$  and temporal spectra  $S(f)$  and structure factors  $S(k)$  (insets) show that the fluctuations increase in power and coherence as  $\Gamma$  increases from 2.2 to 2.6, and at  $\Gamma = 2.8$ , above onset, a coherent square spatial pattern emerges.  $S(k_x, k_y)$ ,  $S(k)$ , and  $S(f)$  have been divided by 10 at  $\Gamma = 2.8$ . The peak in  $S(f)$  at 15 Hz corresponds to the spatial pattern and mixes with the 30 Hz drive frequency to give a peak at 45 Hz. The range of  $k$  in the insets is  $0.16$  to  $6.63 \text{ cm}^{-1}$ ; the structure function peak for  $\Gamma = 2.8$  corresponds to a length of  $0.52 \text{ cm}$ .

yielded fluctuation strengths comparable to those we observe [5,13].

*Local transient waves.*—Transient localized structures oscillating at  $f_d/2$  are visible in Fig. 1(c). Temporal power spectra of the intensity time series for each pixel in the

images are averaged to obtain the power spectra  $S(f)$  shown in Fig. 2. The peak at  $f_d/2$  emerges for  $\Gamma \geq 2$  and increases in power with increasing  $\Gamma$ . The half width at half maximum of the peak, denoted  $1/\tau$ , decreases as  $\Gamma$  increases, indicating increasing temporal coherence of the noisy structures. Except for the peak at  $f_d/2$ ,  $S(f)$  does not depend strongly on  $\Gamma$  for  $\Gamma \geq 2$ . The shape of  $S(f)$  is similar to that for surface excitations (ripples) on a fluid driven by thermal noise [14].

*Fluctuating hydrodynamics.*—The phenomena we have described have the features of noise-driven damped hydrodynamic modes close to a bifurcation as observed in Rayleigh-Bénard convection [5,6], electroconvection [15], and binary-liquid convection [16]. We now interpret the observations using the Swift-Hohenberg (SH) model, which is based on the Navier-Stokes equation with added noise; the model was developed to describe noise near the onset of long-range order in Rayleigh-Bénard convection [8]. Swift-Hohenberg theory predicts that below the onset of ordered patterns, noise drives a ring of modes that increases in power as onset is approached; our observations in Fig. 2 are in qualitative accord with this prediction. The theory also predicts that the nonlinearity of the fluid acting on the noise will lead to an increase of the critical value of the bifurcation parameter for the onset of long-range order. The observations also agree qualitatively with this prediction: for the stainless steel particles the patterns are noisier than those obtained in previous experiments on lead particles, which are more dissipative; further, the onset of long-range order for the stainless steel particles occurs for  $\Gamma \approx 2.77$ , while for lead,  $\Gamma \approx 2.5$  [17]. The granular system is inherently noisy because the number of particles per wavelength is small. Recent experiments have shown that the fluctuations are nearly Gaussian distributed in velocity due to randomization effects from multiple grain-grain collisions during each oscillation cycle [18].

The Swift-Hohenberg model describes the evolution of a spatial scalar field  $\psi(\mathbf{x}, t)$ ,

$$\frac{\partial \psi}{\partial t} = [\epsilon - (\nabla^2 + k_0^2)]\psi - \psi^3 + \eta(\mathbf{x}, t), \quad (1)$$

where  $\epsilon$  is the bifurcation parameter and  $\eta$  is a stochastic noise term such that  $\langle \eta(\mathbf{x}, t)\eta(\mathbf{x}', t') \rangle = 2F\delta(\mathbf{x} - \mathbf{x}')\delta(t - t')$ , where  $F$  denotes the strength of the noise. In the absence of noise ( $F = 0$ ), called the mean field (MF) approximation [8,15], there is an onset of stripe patterns with long-range order at  $\epsilon = \epsilon_c^{\text{MF}} = 0$ . [Our experiments yield squares at pattern onset with slight hysteresis, but we compare our observations to the simplest model for noise interacting with a bifurcation, Eq. (1), which yields stripes at onset via a forward bifurcation; a more complicated model yielding square patterns and hysteresis is described in [19]. For the thin layer of stainless steel particles we did not observe stripe patterns with long-range order for any  $f_d$ .] For  $F \neq 0$ , the

onset of long-range (LR) order is delayed until  $\epsilon = \epsilon_c^{LR} > 0$ , where  $\epsilon_c^{LR} \propto F^{2/3}$ . For  $0 < \epsilon < \epsilon_c^{LR}$ , the pattern is disordered and appears cellularlike [20]. We define the delay in onset as  $\Delta\epsilon_c = \epsilon_c^{LR} - \epsilon_c^{MF}$ .

To compare results from the experiments with results obtained by integration of the SH model, we must first compute the reduced control parameter  $\epsilon = (\Gamma - \Gamma_c^{MF})/\Gamma_c^{MF}$ . However, we have no *a priori* way to determine  $\Gamma_c^{MF}$  since the theory predicts a smooth change in all quantities as the mean field bifurcation is crossed. As in [5], we determine  $\Gamma_c^{MF}$  by varying three parameters to fit the Swift-Hohenberg model to the data:  $\Gamma_c^{MF}$ ,  $F$  [Eq. (1)], and an overall scale factor for the maximum of  $S(k)$ . The resultant shift of  $\epsilon_c^{MF} = 0$  up to  $\epsilon_c^{LR}$  corresponds to a shift from  $\Gamma_c^{MF}$  up to  $\Gamma_c^{LR} = 2.77$ . The three-parameter fit yields  $\Gamma_c^{MF} = 2.64$ , and this gives a delay in onset of  $\Delta\epsilon_c = 0.04$  (Fig. 3).

The noise strength determined from the fit procedure yields  $F = 3.5 \times 10^{-3}$ , which is an order of magnitude larger than in recent experiments on a convecting fluid near a critical point [5] and is a factor of  $10^4$  larger than the noise observed in the experiments of Wu *et al.* [6]. The

theory predicts that at  $\epsilon_c^{LR}$  there should be a jump in  $\langle \psi^2 \rangle$  proportional to  $F^{2/3}$ ; however, the predicted jump, only  $10^{-3}$  in  $\langle \psi^2 \rangle$ , is too small to detect with the precision of our experimental measurements, and, further, such an effect would be masked by the hysteresis in the transition to square patterns.

*Scaling.*—Using the value we have obtained for the reduced control parameter  $\epsilon$ , we can test predictions of scaling given by Eq. (1). Linear theory predicts the following scalings for thermal convection with *small* noise levels near the onset of long-range order: both the noise peak intensity (at the wave number selected by the system) and the correlation time should scale as  $|\epsilon|^{-1}$  and the power in the fluctuations should scale as  $|\epsilon|^{-1/2}$  [4,6]. The scaling behavior found in both the experiment and SH model for large noise levels is shown in Fig. 4, where the

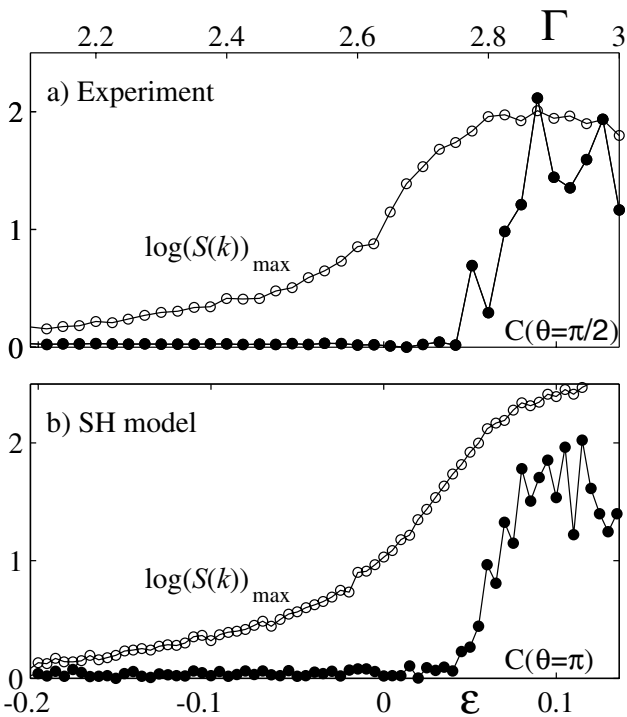


FIG. 3. The growth of the noise power and the onset of long-range order in (a) experiment and (b) the Swift-Hohenberg model. The log of the maximum of  $S(k)$  ( $\circ$ ) increases through the mean field onset ( $\epsilon_c^{MF} = 0$ ), while the onset of long-range order, indicated by the appearance of angular correlations of the radially averaged structure factor [ $C(\theta = \pi/2)$  for the experiment and  $C(\theta = \pi)$  for SH equation ( $\bullet$ )], is delayed to  $\epsilon_c^{LR} \approx 0.04$ . The integration of Eq. (1) uses a scheme described in [21]; the solution is obtained on a  $128 \times 128$  grid with  $k_0 = 1$  and integration time step 0.5.

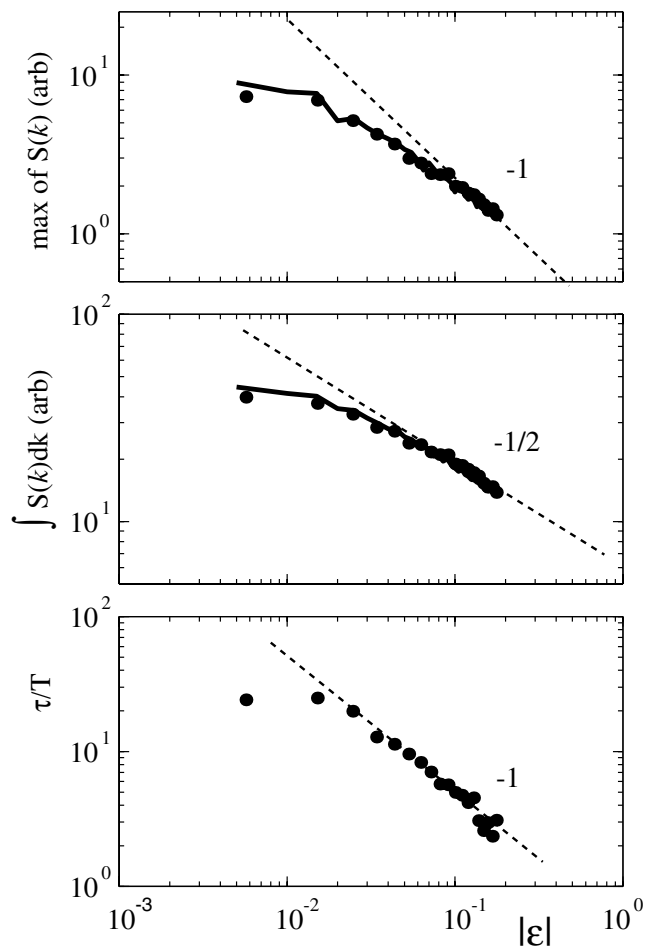


FIG. 4. The noise peak intensity, total noise power, and the noise coherence time  $\tau$  (relative to the oscillation period  $T$ ) as a function of the distance  $\epsilon$  below the onset of patterns. The measured quantities ( $\bullet$ ) compare well to the Swift-Hohenberg equation (solid curve) with  $F = 3.5 \times 10^{-3}$ . Results from both experiment and the SH theory approach the predictions from the linear theory (shown by the dashed lines with the values for their slopes) when  $\epsilon$  is large, far below the onset of long-range order.

noise peak intensity was determined from the maximum of  $S(k)$  (see the insets of Fig. 2), and the power in the fluctuations was determined from the area under the peak in  $S(k)$ , after subtracting the approximately constant background due presumably to incoherent grain noise. The Swift-Hohenberg theory agrees remarkably well with the observations. As expected, both experiment and theory deviate considerably from the linear theory prediction for small  $|\epsilon|$ , where nonlinear effects are large, but for large  $|\epsilon|$  the experiment and simulation approach the scaling predicted by the linear theory. Finally, we have determined from the experimental data the correlation time for the patterns by fitting the  $f_d/2$  peak of  $S(f)$  to a Lorentzian and computing the half width at half maximum,  $1/\tau$ . Again, for large  $\epsilon$  the observations approach the scaling predicted by linear theory but deviate from linear theory for small  $\epsilon$  (Fig. 4).

**Conclusions**—We have shown that a vertically oscillated layer of grains exhibits behavior consistent with the theory of fluctuating hydrodynamics for Navier-Stokes fluids. This indicates that fluctuations must be included in the hydrodynamic equations for granular media [22]. The large fluctuations present in granular fluids suggest that such systems could be useful to study the effects of noise in nonequilibrium fluids *far* below a bifurcation [13,23].

Like numerical studies of elastic gases [24], our experiments and simulations show that fluctuating hydrodynamics can apply down to length scales of only a few mean free paths. Fluctuations are important in fluids at the nanoscale, which are of current interest [25,26]. The fluctuations are difficult to study in gases and liquids but can be studied easily in granular materials, which may demonstrate some essential features of the nanoscale flows.

We thank Guenter Ahlers for helpful discussions and for providing preliminary data. This work was supported by the Engineering Research Program of the Office of Basic Energy Sciences of the U.S. Department of Energy (Grant No. DE-FG03-93ER14312), by The Texas Advanced Research Program (Grant No. ARP-055-2001), and by the Office of Naval Research Quantum Optics Initiative (Grant No. N00014-03-1-0639).

\*Electronic addresses: digoldma@socrates.berkeley.edu  
http://socrates.berkeley.edu/~digoldma

†Electronic address: swinney@chaos.utexas.edu

- [1] L. Bocquet, W. Losert, D. Schalk, T.C. Lubensky, and J.P. Gollub, Phys. Rev. E **65**, 011307 (2001); E.C. Rericha, C. Bizon, M.D. Shattuck, and H.L. Swinney, Phys. Rev. Lett. **88**, 014302 (2002).
- [2] R. Ramírez, D. Risso, R. Soto, and P. Cordero, Phys. Rev. E **62**, 2521 (2000); J.J. Brey, M.J. Ruiz-Montero, and F. Moreno, Phys. Rev. E **63**, 061305 (2001); J. Bougie, S.J. Moon, J.B. Swift, and H.L. Swinney, Phys. Rev. E **66**, 051301 (2002).
- [3] L.D. Landau and E.M. Lifshitz, *Fluid Mechanics* (Pergamon Press, Oxford, England, 1959).
- [4] V.M. Zaitsev and M.I. Shliomis, Zh. Eksp. Teor. Fiz. **59**, 1583 (1970) [Sov. Phys. JETP **32**, 866 (1971)].
- [5] J. Oh and G. Ahlers, Phys. Rev. Lett. **91**, 094501 (2003).
- [6] M. Wu, G. Ahlers, and D.S. Cannell, Phys. Rev. Lett. **75**, 1743 (1995).
- [7] I. Rehberg, S. Rasenat, M. de la Torre Juárez, W. Schöpf, F. Hörner, G. Ahlers, and H.R. Brand, Phys. Rev. Lett. **67**, 596 (1991).
- [8] J.B. Swift and P.C. Hohenberg, Phys. Rev. A **15**, 319 (1977).
- [9] F. Melo, P.B. Umbanhowar, and H.L. Swinney, Phys. Rev. Lett. **75**, 3838 (1995).
- [10] N. Mujica and F. Melo, Phys. Rev. Lett. **80**, 5121 (1998).
- [11] Following [6], we determine intensity fluctuations by subtracting from each measurement the average of 100 images taken at the same phase of the driving cycle.
- [12] As  $\Gamma$  is increased from 2.0g to 2.8g, the wave vector of the dominant mode of the fluctuations smoothly decreases by about a factor of 1.5 as more of the depth of the layer becomes fluidized.
- [13] J. Oh and G. Ahlers, cond-mat/0209104.
- [14] R. H. Katyl and U. Ingard, Phys. Rev. Lett. **20**, 248 (1968).
- [15] M. A. Scherer, G. Ahlers, F. Hörner, and I. Rehberg, Phys. Rev. Lett. **85**, 3754 (2000).
- [16] G. Quentin and I. Rehberg, Phys. Rev. Lett. **74**, 1578 (1995).
- [17] C. Bizon, M. D. Shattuck, J. B. Swift, W. D. McCormick, and H. L. Swinney, Phys. Rev. Lett. **80**, 57 (1998).
- [18] G.W. Baxter and J.S. Olafsen, Nature (London) **425**, 680 (2003).
- [19] H. Sakaguchi and H. R. Brand, Europhys. Lett. **38**, 341 (1997).
- [20] H-W. Xi, J. Viñals, and J.D. Gunton, Physica (Amsterdam) **177A**, 356 (1991).
- [21] M.C. Cross, D. Meiron, and Y. Tu, Chaos **4**, 607 (1994).
- [22] B. Meerson, T. Pöschel, P.V. Sasorov, and T. Schwager, Phys. Rev. E **69**, 021302 (2004).
- [23] J. M. O. de Zárata and J.V. Sengers, Physica (Amsterdam) **300A**, 25 (2001).
- [24] M. M. Mansour, A. L. Garcia, G. C. Lie, and E. Clementi, Phys. Rev. Lett. **58**, 874 (1987).
- [25] J. Eggers, Phys. Rev. Lett. **89**, 084502 (2002).
- [26] M. Moseler and U. Landman, Science **289**, 1165 (2000).